Petr Kulhavy, Martina Syrovatkova, Pavel Srb, Michal Petru, Alzbeta Samkova
Technical University of Liberec, Studentska 2, 461 17, Liberec 1, Czech Republic

Irregular Winding of Pre-preg Fibres Aimed at the Local Improvement of Flexural Properties

Neenakomerno navijanje predhodno impregniranih vlaken za lokalno izboljšanje upogibnih lastnosti

Short Scientific Article/*Kratki znanstveni prispevek*
Received/*Prispelo* 08-2017 • Accepted/*Sprejeto* 10-2017

Abstract

The main undisputed benefit of using long fibre composite materials, whose properties could be targeted for a particular application, lies in the efficient utilisation of material. Using a method of pre-impregnated fibre winding, a rod with a reinforced middle part was created through the local adjustment of the winding angle in order to increase the local bending stiffness. The aim of our work was to describe, experimentally and subsequently using appropriate numerical models, the behaviour of two composite rods, one with a locally variable winding angle and the other with a constant winding angle. The difference in the mechanical behaviour of both structures was clearly evident during the experiment. By using a suitable composite pre-processor and by choosing some multiple element sets, it was also possible to accurately simulate the real behaviour of such components, which actually have several regions, each with different mechanical parameters. Together with the expected different flexural strength, a traditional three-point bending test also explored the different shape of the resulting deformation in the two compared parts. Differences in the maximum strength and the mode of final deformations were also identified.
Keywords: composite, pre-preg, winding, bending, local reinforcement

Izvleček

Največja korist kompozitnih materialov, ojačenih s filamenti, so široke možnosti za učinkovito izrabo materiala, tako da bi bile te lastnosti usmerjene v uporabo za posebne namene. Z uporabo metode navijanja predhodno impregniranih filamentov je bila izdelana palica z ojačenim srednjim delom, kjer je bila za povečanje lokalne upogibne togosti uporabljena možnost lokalne nastavitve kota navijanja. Namen raziskave je bil opisati in preizkusiti primerne numerične modele obnašanja dveh kompozitnih paličastih elementov, enega izdelanega z lokalno spremenljivim kotom navijanja in drugega s stalnim kotom navijanja. Eksperimentalno je bila dokazana razlika v mehanskem obnašanju obeh struktur. Z uporabo ustreznega predprocesorja za definicijo strukture kompozitov in z izbiro večelementnih nizov je bilo mogoče natančno simulirati realno obnašanje komponent z več predeli, od katerih ima vsak drugačne mehanske parametre. Skupaj s pričakovano različno upogibno trdnostjo so bile s tradicionalnim tritočkovnim testom upogibanja proučene tudi različne oblike nastalih deformacij v dveh primerjanih predelih. Ugotovljene so bile tudi razlike v maksimalni trdnosti in obliki končnih deformacij.
Ključne besede: kompozit, predhodno impregnirana vlakna, navijanje, upogibna togost, lokalna ojačitev

1 Introduction

High-strength constructions based on long fibre composite frames are becoming increasingly important across all industrial sectors. Plastic materials reinforced by long fibres are widely used because of their high strength and excellent Young's modulus to density ratio. While conventional materials show one

Corresponding author/Korespondenčni avtor:
Ing. Petr Kulhavý
E-mail: petr.kulhavy@tul.cz

failure mode (i.e. cracking), composites may exhibit one or a combination of failure modes, including fibre rupture, matrix cracking, delamination, interface de-bonding and void growth [1, 2]. Compared to conventional materials, composite laminates offer some unique engineering properties, while presenting interesting and challenging problems for analysts and designers [3]. The aim of this presented work was to study composite rods with local reinforcement achieved through the local varying of the winding angle in chosen layers during manufacturing, and compare it with a constant winding angle. The winding methods were based on the layering of carbon fibres from several spools spinning around a non-bearing core. Information about the optimisation of surfaces created in this way and the associated cross-sections can be found in other works [4, 5]. Zu [4] studied the strain energy criterion in order to create the most appropriate shape of toroidal vessels, achieved through a significantly lower weight and aspect ratio (i.e. the height to width ratio). It was concluded that the structural efficiency of filament-wound material can be determined through a condition of equal shell strains. Blazejewski [5] studied several possible combinations of surface textures and the associated properties that derive from individual plies and the combination of angles. Mertiny [6] studied the dependency of ply angles on the global strength of composite structures, and observed that appropriate structures created using this method are commonly subjected to complex loading conditions.

Modern design software and computer controlled machines allow us to create almost any winding angle (i.e. the angle between the fibre direction and the axis of the mandrel). Fibres may be wound in directions ranging from 0° (axial layering) to 90° (hoop – practically impossible). Computer-controlled winding machines also facilitate the adjustment of the winding angle during an operation. This facilitates the production of multi-angle filament-wound structures. Lea [7] described the benefits of multi-angle winding (e.g. improved tension and bending characteristics) compared with winding at the traditional angle of 54°. This led to significantly higher functional and structural strength under loadings with hoop-to-axial ratios of less than one. However, all of the above mentioned works addressed the idea of a constant angle in each ply. In the presented work, a method based solely on local angle adjustment is introduced.

2 Experimental

2.1 Materials and methods

The used manufacturing method, referred to as winding, is the simultaneous deposition of several filaments, described in the works of Chen [8] or Petru [9]. In our case, carbon pre-preg tapes were used instead of wet fibre filaments. This method of manufacturing parts with rotational shapes from pre-pregs is usually limited only to the straight tubes. The presented method could handle the problem, and through the segmentation of the primary material (i.e. the simultaneously wrapping of up to 20 thin filaments instead of wrapping one wide), we were able to create curved shapes and even parts with fluently changed cross-sections, or to locally change the angles in any place of the part.

The material used was an epoxy UD carbon pre-preg. According to measurements taken, the final thickness after polymerisation was approximately 85% of the original thickness. Pre-preg was produced from reinforced high-strength carbon fibres with a unidirectional orientation (nominal area weight of 150 g/cm^2 and nominal fibre density 180 g/m^3) and epoxy resin. Nominal resin content was 38%, while nominal area weight was 242 g/m^2, using a cure cycle of 60 minutes at 120 °C.

The created tubes were wound from 16 thin tapes and had four plies with a total thickness of 0.84 mm. The fibre layout in the case of the regular rod was 55/-55/55/-55, with a weight of 158 g. In the case of the locally thickened rod, the global layout of the first and fourth plies was also 55/-55/55/-55, while the global layout of the second and third plies in the middle part was locally 55/-70/70/-55, with a weight of 165 g (Figure 1).

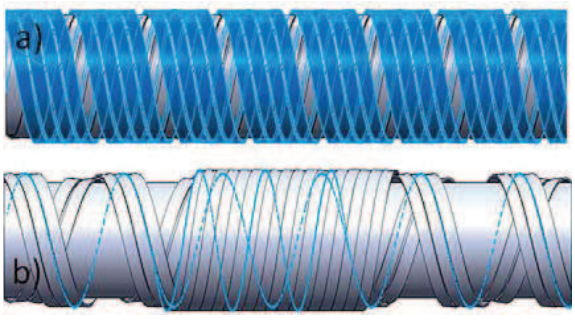

Figure 1: CAD model of fibre layout with visible: a) constant and b) various winding angle

The prediction of mechanical properties of transversely isotropic composites has been the subject of many studies and research in the past, and is also the subject of current research [10–12]. It should be noted that elastic constants are generally different for each type of composite, making it difficult to determine all the constants using analytical models. The stiffness matrix C of one ply in the laminate could be described by equation 1 in the form of expressed engineering constants, where the E_i represents the Young modulus of elasticity in the i-th directions, G_{ij} represents the shear modulus in the ij-plane and μ_{ij} represents *Poisson's* ratio in the specified planes.

$$C = \begin{bmatrix} \frac{1}{E_1} & -\frac{\mu_{12}}{E_1} & -\frac{\mu_{13}}{E_1} & & & \\ -\frac{\mu_{21}}{E_2} & \frac{1}{E_2} & -\frac{\mu_{23}}{E_2} & & & \\ -\frac{\mu_{31}}{E_3} & -\frac{\mu_{32}}{E_3} & \frac{1}{E_3} & & & \\ & & & \frac{1}{G_{23}} & & \\ & & & & \frac{1}{G_{31}} & \\ & & & & & \frac{1}{G_{12}} \end{bmatrix} \quad (1).$$

Because there were several plies with various angles, it was necessary to transform the stiffness matrix of each ply to the final matrix of the entire composite by using equation 2 for individual elements:

$$\begin{aligned}
\overline{C}_{11} &= cos\theta^4 C_{11} + 2cos\theta^2 sin\theta^2 (C_{12} + 2C_{66}) + sin\theta^4 C_{22} \\
\overline{C}_{12} &= cos\theta^2 sin\theta^2 (C_{11} + C_{22} - 4C_{66}) + \\
&\quad + (sin\theta^4 + cos\theta^4) C_{12} \\
\overline{C}_{13} &= cos\theta^2 C_{13} + sin\theta^2 C_{23} \\
\overline{C}_{16} &= cos\theta sin\theta [cos\theta^2 (C_{11} - C_{12} - 2C_{66}) + \\
&\quad + sin\theta^2 (C_{12} - C_{22} + 2C_{66})] \\
\overline{C}_{22} &= sin\theta^4 C_{11} + 2cos\theta^2 sin\theta^2 (C_{12} + 2C_{66}) + cos\theta^4 C_{22} \\
\overline{C}_{23} &= sin\theta^2 C_{13} + cos\theta^2 C_{23} \\
\overline{C}_{26} &= cos\theta sin\theta [sin\theta^2 (C_{11} - C_{12} - 2C_{66}) + \\
&\quad + cos\theta^2 (C_{12} - C_{22} + 2C_{66})] \\
\overline{C}_{33} &= C_{33} \\
\overline{C}_{36} &= sin\theta cos\theta (C_{13} - C_{23}) \\
\overline{C}_{44} &= cos\theta^2 C_{44} + sin\theta^2 C_{55} \\
\overline{C}_{45} &= sin\theta cos\theta (C_{55} - C_{44}) \\
\overline{C}_{55} &= sin\theta^2 C_{44} + cos\theta^2 C_{55} \\
\overline{C}_{66} &= cos\theta^2 sin\theta^2 (C_{11} - 2C_{12} + C_{22}) + \\
&\quad + (sin\theta^2 - cos\theta^2)^2 C_{66} \qquad (2),
\end{aligned}$$

where the line in the upper index represents the element of the transformed matrix and θ represents the angle of direction of individual plies.

The theoretical values of the basic engineering constant after the mutual summing of the individual transformed stiffness matrix for the two concepts of layered rods are presented in polar graphs in Figure 2, one with a constant regular winding angle and the other for the irregular winding angle, reinforced in the centre.

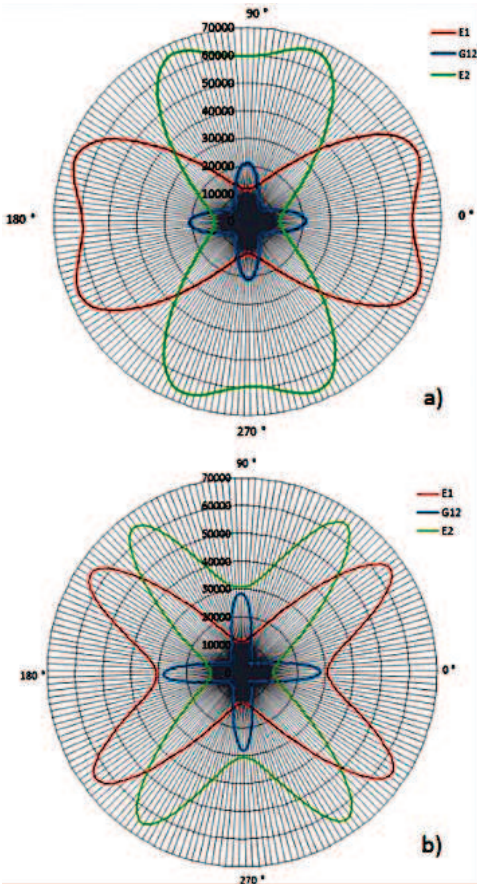

Figure 2: Engineering properties of the a) regular and b) irregular rod

2.2 Experiment

The flexural strength of a material is the maximum stress that a material subjected to bending load is able to resist before failure. A traditional three-point bending test was used to compare the homogenous and locally variable tube. A hydraulic circuit with an

attached force-meter and a cylindrical indenter were used as the source of the loading force. The use of a hydraulic system is particularly advantageous with regard to constant speed regulation, shock absorption and the smoothness of movement without "jumps" that are typical, for example, for pneumatic systems due to the compressibility of the used medium. Devices based on electric power are usually limited by their size and the range of the operating values. The applied quasi static loading was increased in increments of 0.5 mm/s until it caused the final displacement of the used indenter of 40 mm or until total failure of the tested samples occurred. It is evident from the pictures in Figure 3 that the two types of rods showed significantly different shapes of deformation during loading. The distance between the supports was 380 mm in this case.

It is possible to determine flexural stress based on the measured deformation and force response (equation 3, where D and d [m] represent the outer and inner tube diameters, F [N] represents the maximal bending force and l [m] represents the distance between supports). It should be emphasised that it is not possible to use the additive law for the cross section module W_o, simply using the difference of values of individual diameters.

$$\sigma_o = \frac{M_{omax}}{W_o} = \frac{8\,D\,F_{max}\cdot l}{\pi(D^4 - d^4)} \tag{3}$$

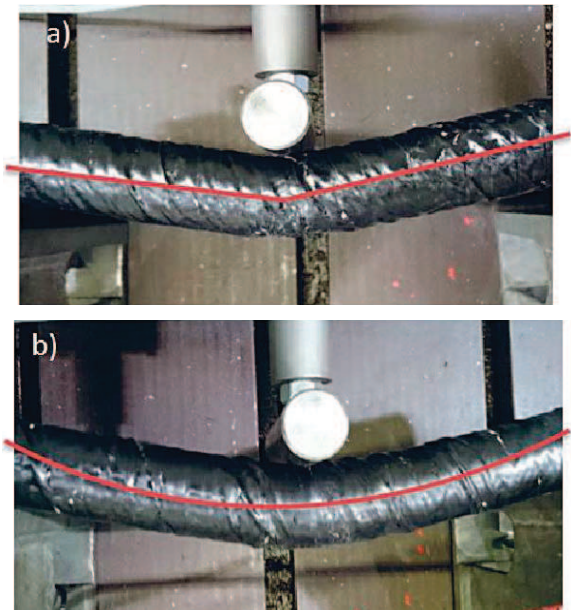

Figure 3: Shape of deformation during the bending test for: a) homogenous and b) locally reinforced rod

2.3 Model

The prediction of the behaviour of composite materials is a very complex problem because the process induces the orientation of fibres, the interface of plies, etc. The finite-element method (FEM) is a powerful tool, without which it is impossible to efficiently design composite parts today. Numerical analysis allows us to derive the different strain energies stored in the material directions of the constituents of composite materials [13]. In our case, the models of the shell composite plate of the two tubes were created using an ANSYS ACP pre-post processor. The model was solved as a fully contact task. The pure penalty formulation with the nodal-normal detection of integration points was used for the combination of solid and shell elements. Frictional support with asymmetric behaviour was also set.

The simplest way of handling an initially unconstrained model (i.e. a rod simply lying on solid supports) was to add weak springs as mentioned by Gruber or Whitney [14, 15]. The spring constant was dependent on the loading parameter, thus the effect could only be seen in the beginning of the simulation. The scheme of the created model with boundary conditions is shown in Figure 4, which also presents the results of equivalent stress in the simulation of the regularly wound tube (±55°).

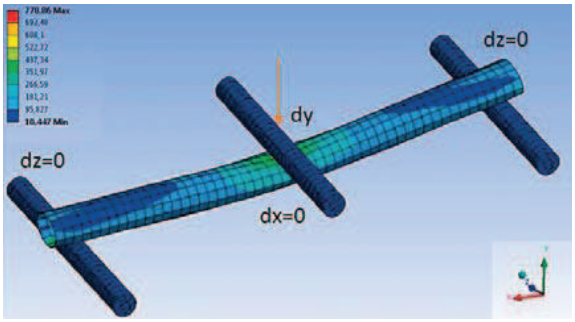

Figure 4: Layout of the solved shell/solid model (results of stress distribution for regular winding)

The irregular winding (local reinforcement) in the middle third of the modelled rod was created using a combination of several local coordinate rosettes and oriented elements sets. In order to double the density of the central laminate, the deflection of the inner rosette BETA is equal to equation 4:

$$\beta = \frac{\frac{\pi}{2} - \alpha}{2} \tag{4},$$

where alpha represents the global winding angle relative to the actual central axis.

The computed values for both cases are illustrated in Figure 5, while the reference vectors in the second ply of the model can be seen in Figure 6.

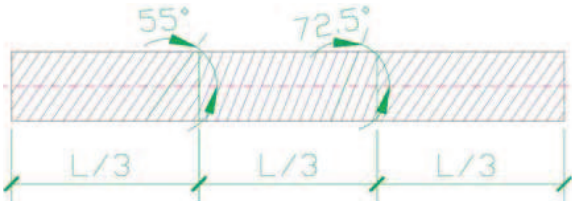

Figure 5: Scheme of ply orientation with an irregular centre part

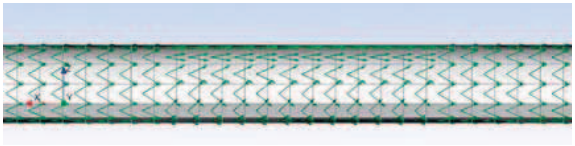

Figure 6: Reference directions in one of the elementary plies in the created FEM model

The eventual drop-off places in the boundaries between the various sectors was filled by material with the same properties as the primary composite in order to simplify the model solution. The equivalent stress in the entire locally reinforced rod can be seen in Figure 7.

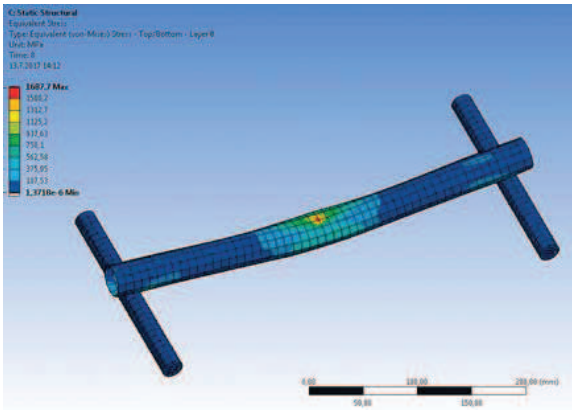

Figure 7: Equivalent stress distribution in the irregularly wound rod

3 Results and discussion

Behaviour in terms of the flexural loading of both types of rods was experimentally measured and simultaneously modelled. Experimental results are shown in Figure 8. Even if the values of the maximum forces are almost the same, the distinctly different course of displacement could be seen. While the ruptures and delamination were fluent in the case of the regular rod, the reinforced rod was extremely durable until the final moment of sudden total collapse.

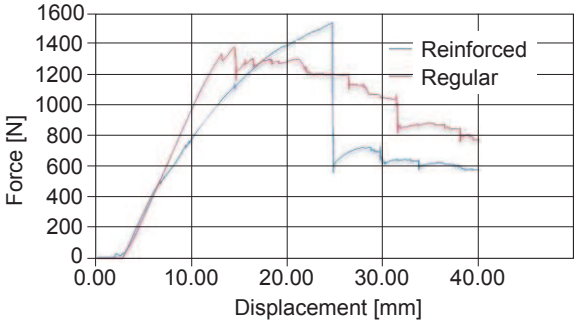

Figure 8: Graph of experimental results of the bending test for: a) regular and b) reinforced rods

Basic statistics from the resultant bending stress and absolute deformation in the direction of the acting load are presented in Table 1 below for several created samples.

Table 1: Experimental results of the three-point bending test

Sample	Stress, σ [MPa]		Deformation, d_y [mm]	
	$\overline{x}$	μ	$\overline{x}$	μ
Regular	768.41	59.08	14.25	1.73
Reinforced	930.39	28.58	26.00	1.83

The results obtained in the created model (Figure 9) showed similar trends for approximately the first 10 mm of deformation. This is also the point where the results of our experiment start to differ significantly.

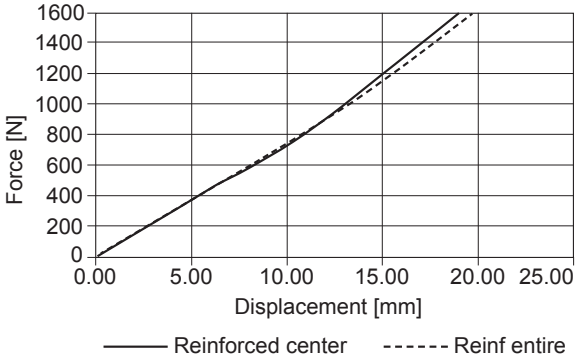

Figure 9: Graph of the model results of the bending test for: a) regular and b) reinforced rods

The following course, in which several different deviations occurred, could not be simply explained by the stress/strain relationship for the reinforced layered material. We therefore performed a model comparison of occurring failure criteria.

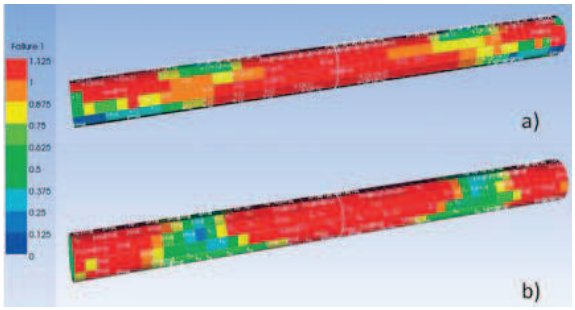

Figure 10: Tsai-Hill and Puck failure criteria in a) regular and b) irregular rods

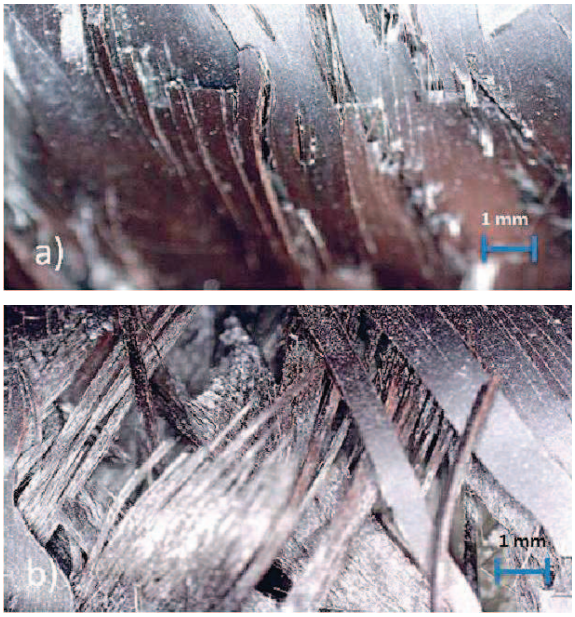

Figure 11: Micro-pictures of the place of rupture in the centre of a rod: a) regular b) irregular winding angle

One of the chosen criteria was Tsai-Hill. Capela, for example, studied this criterion in bending and torsion loading in his work [16]. He claimed that the Tsai-Hill criterion could sufficiently predict the loading effect on the static strength of specimens. The second criterion used was the Puck criterion, which is probably the most frequently used criterion today because of its universal application. Quite interesting research was conducted in this field by Francis [17] who stated that the matrix shear or tension cracking modes were always observed in the first ply for carbon/epoxy thin-walled tubes with $[0/90]_s$ and $[\pm 45]_s$. It is evident from Figure 10 that the modes of the layer failure are slightly different. In Figure 10b, the "undamaged" green elements are precisely in the location of the supports and all other elements of the composite rod are fully loaded. In the case of ultimate loading, this means that the stress will be still transferred through the entire part, not just locally, as could be seen in Figure 3a. This is the right way to create composite parts because there is no reason to use reinforced composite materials when the concentration of acting stresses is not high.

4 Conclusion

The unconventional method of pre-preg winding was introduced in the first part of this study. Even if there are numerous benefits (compared to traditional "wet" methods), the main problem lies in the fact that the stickiness of material causes a significant increase of forces in the entire mechanism and the occurrence of the imperfect alignment of fibres and their mutual storage in several places.

The aim of this study was to use this method to create and subsequently compare the behaviour of two rods, one with a regular winding angle in all plies and the other locally reinforced by local adjustments to the angle in two of the four total plies. During our experiment, we identified a significantly different behaviour between the two types of rods tested, particularly at the moment of part rupture. The experimental results were evaluated using a numerical model, applying an advanced composite pre-post processor. Based on the work performed, we can conclude that local changes in the winding angle may not only locally increase (or decrease) flexural strength, but may also change the shape of part deformation and the resulting material failure process (Figure 11). Through the targeted local adjustment of the winding angle, it is possible to save the material and concentrate it solely in places that actually require reinforcement. This could be seen, for example, in Figure 10, which illustrates a mutual comparison of failure criteria. This is one of the most important findings of our work, as one of the basic principles of designing composite structures is to provide fibres only where are they need.

The presented work introduced a topically important area in the field of advanced high-strength materials.

Future work will concentrate not only on straight tubes, but also on certain curved and closed composite frames. The question of how to adequately describe imperfections in layered plies, such as the wrapping and twisting of the fibres, remains unanswered.

Acknowledgement

The results of this project (LO1201) were made possible with co-funding from the Ministry of Education, Youth and Sports, as part of targeted support from the programme "Národní program udržitelnosti I".

References

1. AZZAM, A., LI, W. An experimental investigation on the three-point bending behavior of composite laminate. *IOP Conference Series: Materials Science and Engineering*, 2014, **62**, doi: 10.1088/1757-899x/62/1/012016.
2. SUGANUMA, Yusuke, FUKUDA, Hiroshi. Applicability of compression bending test to measure compressive failure strain. *16th Internatonal Conference on Composite Materials*, 2007, Kyoto, Japan. Available on World Wde Web: <http://www.iccm-central.org/Proceedings/ICCM16proceedings/contents/pdf/WedB/WeBM1-04-ge_suganumay226733.pdf>.
3. KHERREDINE, L., GOUASMI, S., LAISSAOUI, R., ZEGHIB, N. E. Evaluation and measurement of the damping properties of laminated CFRP composite plate. *IOP Conf. Series: Materials Science and Engineering*, 2012, **28**, doi: 10.1088/1757-899X/28/1/012021.
4. ZU, Lei, KOUSSIOS, Sotiris, BEUKERS, Adriaan. Optimal cross sections of filament-wound toroidal hydrogen storage vessels based on continuum lamination theory. *International Journal of Hydrogen*, 2010, 35(19), 10419–10429, doi: 10.1016/j.ijhydene.2010.07.142.
5. BLAZEJEWSKI, Wojciech. *Kompozytowwe zbiorniki wysokocisnieniowe wzmocnione wloknami wedlug wzorow mozaukowych. Wrocław:* Oficyna Wydawnicza Politechnki Wrocławs, 2013.
6. MERTINY, P., ELLYIN, F., HOTHAN, A. An experimental investigation on the effect of multi-angle filament winding on the strength of tubular composite structures. *Composites Science and Technology*, 2004, 64(1), 1–9, doi: 10.1016/s0266-3538(03)00198-2.
7. LEA, Richard H., YANG, Chihdar. Improving the mechanical properties of composite pipe using multi-axial filament winding. *Proceedings of NACE Annual Conference Corrosion,* 1998, San Diego, California: CE International.
8. CHEN, Weiming, YU, Yunhua, LI, Peng, WANG, Chengzhong, ZHOU, Tongyue, YANG, Xiaoping. Effect of new epoxy matrix for T800 carbon fiber/epoxy filament wound composites. *Composites Science and Technology*, 2007, **67**(11–12), 2261–2270, doi: 10.1016/j.compscitech.2007.01.026.
9. PETRU, Michal, MARTINEC, Tomas, MLYNEK, Jaroslav. Numerical model description of fibres winding process for new technology of winding fibres on the frames. *Manufacturing Technology*, 2016, **16**(4), 778–785.
10. CHAMIS, C. C. Mechanics of composite materials: past, present, and future. *Journal of Composites, Technology and Research*, 1989, **11**(1), 3–14, doi: 10.1520/ctr10143j.
11. YOUNES, Rafic, HALLAL, Ali, FARDOUN, Forouk, CHEHADE, Fadi Hajj. Comparative review study on elastic properties modeling for unidirectional composite materials. In *Composites and Their Properties*, 2012, Rijeka : INTECH, doi: 10.5772/50362.
12. HASHIN, Zvi, ROSEN, B. Walter. The elastic moduli of fiber reinforced materials. *Journal of Applied Mechanics*, 1964, **31**(2), 223, doi: 10.1115/1.3629590.
13. KULHAVY, Petr, LEPSÍK, Petr. Digitization of structured composite plates with regard to their numerical simulations. *Manufacturing Technology*, 2017, **17**(2), 198–203.
14. GRUBER, G., WARTZACK, S. Three-point bending analyses of short fiber reinforced thermoplastic: a comparison between simulation and test results. *SASTech Journal*, 2013, **12**(1), 1–8.
15. WHITNEY, J. M. Shear correction factors for orthotropic laminates under static load. *Journal of Applied Mechanics*, 1973, **40**(1), 302, doi: 10.1115/1.3422950.
16. CAPELA, C., FERREIRA, J. A. M., FEBRA, T., COSTA, J. D. Fatigue strength of tubular carbon fiber composites under bending/torsion loading. *International Journal of Fatigue*, 2015, **70**, 216–222, doi: 10.1016/j.ijfatigue.2014.09.008.
17. FRANCIS, Philip H., WALRATH, David E., WEED, Donald N. First ply failure of G/E laminates under biaxial loadings. *Fiber Science Technology*, 1979, **12**(2), 97–110, doi: 10.1016/0015-0568(79)90023-X.